Effects of localized phonons on interfacial thermal conductance

Hangbo Zhou, Gang Zhang, and Yong-Wei Zhang*
*Institute of High Performance Computing, A*STAR, Singapore 138632, Singapore*

(Received 1 July 2022; revised 2 November 2022; accepted 14 November 2022; published 30 November 2022)

Interfacial thermal conduction is traditionally described by the transmission of traveling phonons in their bulk counterparts. However, recent experiments suggest that localized phonons at an interface may exert a substantial influence on interfacial thermal conductance. By considering quantum phonon scattering processes at a weakly interacting interface, we analyze the role of localized phonons at the interface involved in the interfacial thermal conduction and discover that there is a coupling between traveling phonons and the even orders of the localized phonons at the interface. Using fourth-order localized phonons as an example, we show that the traveling phonons can collide with the localized phonons at the interface. Such collisions can significantly change the transmission probability of the traveling phonons and thus affect the interfacial thermal conductance, and importantly, such effects become increasingly significant with increasing temperature.

DOI: 10.1103/PhysRevB.106.195435

I. INTRODUCTION

Interfaces play a critical role in the thermal management of nanoscale devices [1–4]. The prediction of interfacial thermal conductance requires an understanding of phononic properties and their scattering mechanisms at the interface. Due to the breakdown of translational symmetry and peculiar interatomic interactions at the interface, the phonon modes at an interface may differ significantly from their bulk counterparts [5,6]. Depending on the nature of the phonons, their modes can be classified into extended (or traveling) modes and localized modes [6]. The extended modes involve lattice vibrations on both sides. Their contribution to interfacial thermal conductance can be described by using the phonon gas model [7] or nonequilibrium Green's function (NEGF) formalism [8–10] under the assumption that the phonon transport is described by the probability of phonon transmission across the interface. On the other hand, due to the breakdown of periodicity and abrupt change in potential, phonons can be easily localized at the interface [4,11]. The localized phonons are spatially confined at the interface, and their carried energies are not propagating. It is commonly believed that they are not energy carriers and thus do not contribute to the thermal transport processes. Compared with the extended modes, localized modes draw much less attention.

However, recent experiments surprisingly showed that the localized phonon modes at an interface could have a substantial influence on the interfacial thermal conductance [12,13]. It was suggested that the localized interfacial modes could act as a bridge to mediate the transport of bulk modes [14,15]. In addition, molecular dynamic simulation also suggested that the localized modes at the interface could play an important role in the interfacial thermal conductance [16,17]. We note that although those experimental and theoretic studies presented convincing evidence of the strong effects of localized phonon modes on interfacial thermal conductance, the underlying mechanisms for the strong effects so far remain unclear.

In this work, we consider a weakly interacting interface and formulate a quantum phonon-scattering model to analyze the effects of localized phonons on interfacial thermal conductance. In order to describe the localized phonon modes and phonon-phonon interactions, a nonlinear interatomic potential is taken to describe the interatomic interaction at the interface, which enables the creation of localized phonon modes. Through the fourth-order interatomic interface, we are able to consider the interactions between the traveling phonons and localized phonons. We find that a localized phonon can merge with a traveling phonon from one side and then emit the traveling phonon into the other side of the interface while keeping the localized phonon on the original side. Through this process, localized phonons are able to catalyze the transport of traveling phonons and thus affect interfacial thermal transport. Hence, the present work unveils the underlying mechanisms for the interactions between traveling and localized modes at the interface and explains the role of localized modes in the interfacial thermal conduction observed in experiments.

II. THEORETICAL DERIVATION

We model a weakly interacting interface that connects two harmonic leads by using nonlinear interfacial coupling. In general, the Hamiltonian can be written as

$$H = H_L + H_R + H_{\text{int}}, \tag{1}$$

where $H_L = \sum_q \frac{(\tilde{p}_q^L)^2}{2m} + \frac{1}{2}\omega_q^2(\tilde{x}_q^L)^2$ and $H_R = \sum_q \frac{(\tilde{p}_q^R)^2}{2m} + \frac{1}{2}\omega_q^2(\tilde{x}_q^R)^2$ are collections of harmonic oscillators. We consider an interface at which nonlinear phonon scattering contributes significantly to interfacial thermal conductance. So the interaction Hamiltonian H_{int} includes a nonlinear potential

*zhangyw@ihpc.a-star.edu.sg

term that causes multiple-phonon scattering processes in general. In order to explore in detail how the nonlinearity in the interface potential gives rise to the phonon-phonon scattering, a common approach is to expand the potential with respect to the atomic displacements so that we can analyze the multiple-phonon scattering processes order by order. The first-order term vanishes as the atoms vibrate at the equilibrium positions. The second-order term contributes to the elastic phonon scattering that accounts for phonon transmission and backscattering. The lowest-order term accounting for the phonon-phonon scattering is the third-order term, which describes phonon merging, splitting, emission, and reflection. However, it is impossible for the localized phonon involved in the three-phonon processes to contribute to interfacial thermal conductance without changing its phonon states. Hence, the fourth-order term is the lowest-order term for which localized phonons are possibly involved in the phonon-phonon scattering processes. For example, a localized phonon at the interface may absorb a traveling phonon from lead L and then emit a phonon to lead R, with the original phonon remaining intact at the interface. Therefore, the minimum Hamiltonian required to take into account the effects of localized phonons on the interfacial thermal conductance should include the fourth or even higher order of nonlinearity in the potential. With this concern, our interaction Hamiltonian contains interatomic potentials up to the fourth order as

$$V = \frac{1}{2!}\sum_{ij} K_{i,j}x_i x_j + \frac{1}{3!}\sum_{ijk}(V_{ij,k}x_i x_j x_k + V_{i,jk}x_i x_j x_k) + \frac{1}{4!}\sum_{ijkl}(T_{ijk,l}x_i x_j x_k x_l + T_{ij,kl}x_i x_j x_k x_l + T_{i,jkl}x_i x_j x_k x_l),$$

where the matrix K is the interatomic force constants (IFCs) of quadratic coupling, the tensors V are the IFCs of cubic coupling, and the tensors T are the IFCs of the fourth-order coupling. Here, we place the subindices of the left-lead side to the left of the comma, while the subindices of the right lead are to the right of the comma. The displacement operators at the interface, for example, x_i^L, can be expanded with respect to the displacement of the normal modes of phonons with wave vector q in L as $x_i^L = \sum_q c_i^q \tilde{x}_q^L$.

For the calculations of thermal current, we employ the formalism developed in Ref. [18] under the assumption that the interfacial coupling is weak. In this weak-interaction regime, the thermal current is determined by the correlations of the operators that are involved in the interface coupling. For example, the contribution of quadratic coupling can be written as

$$I_{2p} = -\frac{1}{4\hbar}\sum_{ij,kl} K_{i,j}K_{k,l}\int_{-\infty}^{\infty}\Psi_{ik}(t)\Phi_{jl}(t)dt, \qquad (2)$$

where $\Psi_{ij}(t) = \frac{d\Phi_{ij}(t)}{dt}$ and $\Phi_{ij}(t) = \langle x_i(t)x_j\rangle$ are the two-point displacement correlation functions. The two-point correlation functions can be written in terms of the spectral densities of the left part Γ_L and right part Γ_R as $\Phi_{ij}(t) = \int_{-\infty}^{\infty}\frac{d\omega}{\pi}\Gamma_{ij}(\omega)n(\omega)e^{i\omega t}$ and $\Psi_{ij}(t) = i\int_{-\infty}^{\infty}\frac{d\omega}{\pi}\Gamma_{ij}(\omega)\omega n(\omega)e^{i\omega t}$. A straightforward derivation shows that Eq. (2) can be cast into the Landauer formula,

$$I_{2p} = \frac{1}{(2!)^2}\sum_{ijkl} K_{i,j}K_{k,l}H_{ikjl}, \qquad (3)$$

where

$$H_{ikjl} = \frac{4}{\hbar}\int_0^{\infty}\frac{d\omega}{\pi}\omega J_{ik}^L(\omega)J_{jl}^R(-\omega)[n^L(\omega) - n^R(\omega)]. \qquad (4)$$

This result can also be derived from the NEGF approach developed in the literature [19]. It is well known that the quadratic coupling between the two leads causes only elastic scattering processes and its contribution to interfacial thermal conductance can be estimated through the phonon transmission function of these extended phonon modes.

The elastic phonon scattering processes are phenomenologically shown in Figs. 1(a) and 1(b). Here, we focus on a phonon with a specific frequency ω. It should be noted that the phonon energy and phonon frequency will not change during the elastic scattering. The atoms labeled 1 and 2 are the interfacial atoms that involve interactions with atoms on their own side of the interface. The coupling between atoms

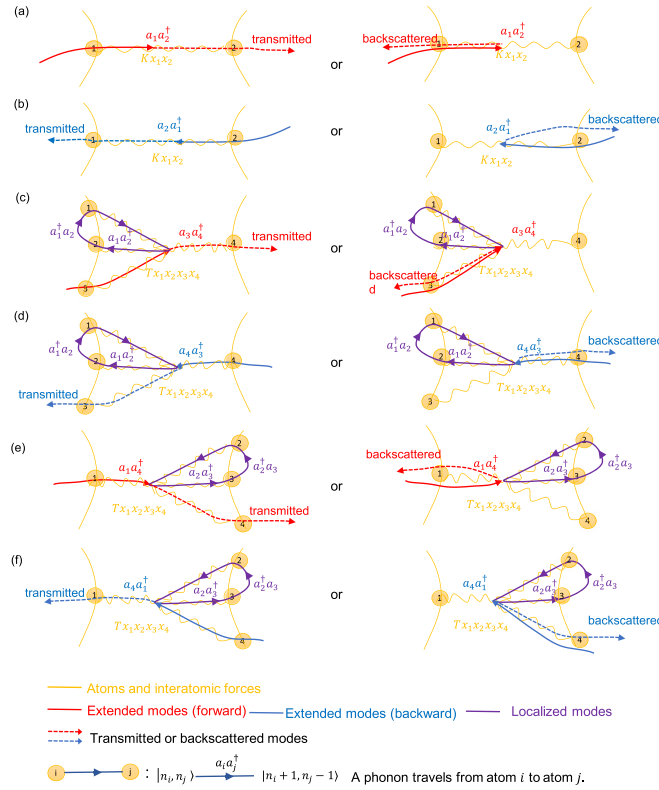

FIG. 1. Schematic illustration of elastic phonon scattering caused by atoms that involve (a) and (b) quadratic couplings and (c)–(f) fourth-order couplings. The orange symbols and lines denote the atoms and their interatomic forces, respectively. The red lines denote the forward-scattering process of extended modes, the blue lines denote the backward-scattering process of extended modes, and the purple lines denote the localized phonon modes. The dashed line represents either a transmitted phonon or a backscattered phonon. Atoms labeled differently can be the same atom physically if they are on the same side of the interface.

1 and 2 is of quadratic order. Through the coupling, there are probabilities that a phonon of energy $\hbar\omega$ can be annihilated at atom 1 and, simultaneously, a phonon of the same energy can be created at atom 2 and then thermalized into the right lead. Through this process, an energy of amount $\hbar\omega$ is transmitted across the interface. There are also probabilities that it is backscattered into atom 1 and then thermalized into the left lead. As required by detailed balance, a phonon may also experience a backward-scattering process, as shown in blue in Fig. 1(b), where a phonon of energy $\hbar\omega$ is transmitted from atom 2 to atom 1. During the cycles of phonon creation and annihilation between atoms 1 and 2, phonons are either dissipated into or emitted from the baths of both sides. The amount of net heat flow is determined by the competition between the phonon emission and dissipation rates of both baths.

For third-order coupling, we have shown that it contributes to three-phonon processes, which consist of phonon splitting, merging, partial reflection, and partial transmission [18,20]. However, in all three-phonon processes, all the phonons are not conserved. They are either destroyed or newly created in the scattering process during thermal transport. Therefore, the localized phonons are not involved. In other words, third-order coupling contributes to only three-phonon scatterings between the traveling phonons, and its coupling order is not high enough to consider interactions between the localized phonons and traveling phonons. We will show that the latter interaction is rooted in the fourth-order interatomic potential.

It is known that the fourth-order coupling contributes to the four-phonon processes, which may involve processes of a single phonon splitting into three phonons or three phonons merging into one or two phonons merging together with the emission of two new phonons. However, surprisingly, in addition to the normal four-phonon processes, we find a special kind of four-phonon process, as illustrated in Figs. 1(c)–1(f), can interact with traveling phonons. For example, in Fig. 1, a phonon mode from atom 3 collides with a phonon from vibrations between atoms 1 and 2 on the left side of the interface, and then it can emit the *original* phonon to atoms 1 and 2 and another phonon to atom 4. Here, the vibrations between 1 and 2 are localized phonons since they do not travel across the interface. On the other hand, the vibrations between 3 and 4 are extended or traveling phonons as they travel across the interface. This four-phonon process can be described as a collision between the extended modes and localized modes. Below, we will show that the existence of such collisions will substantially affect the transmission of the extended modes.

Mathematically, such collisions come from both the cross term between quadratic and fourth-order couplings and the fourth-order couplings themselves. To calculate the thermal current, one needs to consider the net heat flow from all the combinations between a forward process [Figs. 1(a), 1(c) and 1(d)] and a backward process [Figs. 1(b), 1(d) and 1(f)]. Except for the process in Figs. 1(a) and 1(b), they all involve the contribution of localized phonons. In the following, we analyze these processes in details.

We first analyze the contribution of the correlation between the term $\sum_{ij} K_{i,j}x_i x_j$ and the term $\frac{1}{4!}\sum_{ijkl} T_{ijk,l}x_i x_j x_k x_l$, where the forward process is mediated via the coupling of $\sum_{ij} K_{i,j}x_i x_j$ while the backward process is mediated via the coupling $\frac{1}{4!}\sum_{ijkl} T_{ijk,l}x_i x_j x_k x_l$ [Figs. 1(a) and 1(d)]. The evaluation of this term involves the calculation of the four-point correlation function. By using Wick's theorem, we can find that

$$\phi^L_{ijkl}(t) = \langle x_i(t)x_j x_k x_l\rangle = c^L_{ij}(t)Z^L_{kl} + c^L_{ik}(t)Z^L_{jl} + c^L_{il}(t)Z^L_{jk},$$

where $c_{ij}(t) = \langle x_i(t)x_j(0)\rangle$ are the displacement-correlation functions and we have defined $Z_{ij} = \langle x_i x_j\rangle = c_{ij}(0)$ as the correlation functions when $t = 0$. If $i = j$, it is the expectation value of the square of the amplitude of atomic vibration. Therefore, it increases with temperature as well as the spectral density of that atom. In the high-temperature limit, it should be proportional to temperature according to the equal-partition theorem.

With the correlation function, we find that its contribution to the thermal current is

$$I_h = \frac{1}{2!}\frac{1}{4!}\sum_{ijklmn} 6K_{i,j}T_{klm,n}Z^L_{lm}H_{ikjn}. \tag{5}$$

We immediately find that its contribution to the thermal current is proportional to Z^L, which provides an extra temperature-dependent component. As we know, H_{ikjn} will saturate in the high-temperature limit. So this term will eventually linearly increase with temperature.

This phonon scattering process can be phenomenologically explained through the scattering process shown in Fig. 1. It describes a combination of two cycles of scattering processes. In the first cycle, the forward process is carried out through the quadratic coupling [Fig. 1(a)], and the backward scattering is through the fourth-order coupling [Fig. 1(d)]. In this backward-scattering process, the transmitted phonon maintains its energy across the interface. So it is regarded as elastic scattering with an extended mode. This happens when the vibrations of the other two atoms that involve in the fourth-order coupling, atoms 1 and 2, are in a localized phonon mode, such that the phonon forms a closed cycle on the left side and does not travel to the other side of the interface. However, whenever an elastic scattering from atom 4 to atom 3 happens, a phonon conversion simultaneously occurs between atoms 1 and 2 due to the fact that their interatomic coupling is in the fourth order. In such a way, the localized phonon between atoms 1 and 2 will affect the scattering probability between atoms 3 and 4 and thus influence the interfacial thermal conduction. We note that atoms 1 and 2 can physically be the same atom. In such cases, the creation and annihilation processes at atom 1, although they do not affect the vibrational state of atom 1, will simultaneously trigger the transmission processes of traveling phonons between atoms 3 and 4 and thus affect the interfacial thermal conductance. This effect is quantitatively described by the quantity Z^L. In the other cycle, on the other hand, the forward process is carried out by the fourth-order coupling [Fig. 1(c)], and the backward process is carried out by the quadratic coupling [Fig. 1(b)]. Similarly, the direction of the net heat flow is determined by the phonon emission and dissipation ratio of the two baths.

Above, we showed a typical example in which a high-order potential can cause phonon scattering mediated by localized phonons. In a similar manner, we can also calculate the

other contributions. Next, we consider the cross term between $\sum_{ij} K_{i,j}x_i x_j$ and $\frac{1}{4!}\sum_{ijkl} T_{i,jkl}x_i x_j x_k x_l$. The thermal current turns out to be

$$I_h = \frac{1}{2!}\frac{1}{4!}\sum_{ijklmn} 3K_{i,j}T_{k,lmn}Z^R_{mn}H_{ikjl}. \tag{6}$$

Its phenomenological illustration can also be described by two cycles: The first one is illustrated in Figs. 1(a) and 1(f), and the second one is illustrated in Figs. 1(b) and 1(e). We find that the second term depends on Z^R. This term together with the first term causes an asymmetry between the left and right baths, resulting in a thermal rectification effect under a temperature bias.

Our calculation shows that the cross term between $\sum_{ij} K_{i,j}x_i x_j$ and $\sum_{mnop} T_{mn,op}x_m x_n x_o x_p$ does not contribute to the thermal current since a closed cycle cannot be formed.

So far, we have analyzed the cross term between the quadratic and fourth-order couplings. We show that the cross term increases linearly with temperature in the high-temperature limit. Next, we work on the terms coming solely from the fourth-order coupling. We first analyze the term from the coupling between $T_{ijk,l}$ and $T_{mno,p}$. We find that such coupling contributes not only to the four-phonon process but also to the elastic scattering process. Its contribution to the elastic scattering process is illustrated through cycles shown in Figs. 1(c) and 1(d). In this case, two localized phonons form on the left side, which affects both the forward and backward processes. Mathematically, its contribution to the thermal current is given by

$$I_{h(2p)} = \frac{1}{(4!)^2}\sum_{ijklmnop} 9T_{ijk,l}T_{mno,p}Z^L_{ij}Z^L_{no}H_{kmlp}. \tag{7}$$

We find that the thermal current depends on the second order of Z and increases quadratically with increasing temperature in the high-temperature limit. Similarly, the contribution from the coupling between $T_{l,ijk}$ and $T_{p,mno}$ is

$$I_{h(2p)} = \frac{1}{(4!)^2}\sum_{ijklmnop} 9T_{l,ijk}T_{p,mno}Z^R_{ij}Z^R_{no}H_{lpkm}, \tag{8}$$

and it is illustrated in Figs. 1(e) and 1(f). The contribution from coupling between $T_{ijk,l}$ and $T_{m,nop}$ is

$$I_{h(2p)} = \frac{1}{(4!)^2}\sum_{ijklmnop} 9T_{ijk,l}T_{m,nop}Z^L_{ij}Z^R_{op}H_{kmln}, \tag{9}$$

and the scattering processes are illustrated in Figs. 1(c) and 1(f) and 1(d) and 1(e). We also find that cross term between $\sum_{ijkl} T_{ij,jk}x_i x_j x_k x_l$ and $\sum_{mnop} T_{mn,op}x_m x_n x_o x_p$ does not contribute to the elastic scattering. In this case, only the four-phonon processes contribute to phonon transport. These localized phonons are not able to affect the phonon transport processes.

Now, we have evaluated all the combinations. By defining

$$S^L_{ij} = \sum_{mn\in L} T_{imn,j}Z^L_{mn}, \quad S^R_{ij} = \sum_{mn\in R} T_{i,mnj}Z^R_{mn}, \tag{10}$$

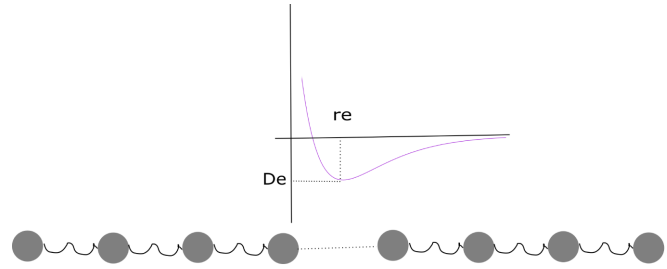

FIG. 2. Illustration of the setup used in the calculation. The interface is modeled by the Morse potential, which has a minimum energy of D_e at the equilibrium position r_e. The left and right leads are assumed to be Rubin baths.

the total thermal current can be written in a concise form as

$$I_{h(2p)} = \sum_{ij,kl} H_{ijkl}\left(\frac{1}{2!}K_{ik} + \frac{3}{4!}\left(S^L_{ik} + S^R_{ik}\right)\right) \times \left(\frac{1}{2!}K_{jl} + \frac{3}{4!}\left(S^L_{jl} + S^R_{jl}\right)\right). \tag{11}$$

We have shown that the fourth-order coupling at the interface can influence the transmission of extended modes. By making a comparison with Eq. (2), we find that the temperature-dependent quantity S can be regarded as an effective quadratic force constant. The value of S increases linearly with temperature. Therefore, this effect will increase with the increase in temperature and will eventually become dominant in the high-temperature regime. This finding suggests that to calculate the thermal current across a weakly interacting interface, it is insufficient to consider only the quadratic interatomic force constant K. It is necessary to evaluate the effective force constant S that includes the contribution from the fourth-order potential, which essentially considers the localized phonons. This is particularly important at higher temperatures as the impacts from localized phonons are stronger.

III. NUMERICAL RESULTS OF AN APPLICATION

Next, we use a one-dimensional chain to demonstrate this effect. In the simplest model, the interface connects two Rubin baths, as shown in Fig. 2. At the interface, only the nearest atoms interact with each other. The interatomic force constant within the bath is characterized by k. At the interface, we use Morse potential $V(r) = D_e(e^{-2a(r-r_e)} - 2e^{-a(r-r_e)})$ to simulate the coupling potential between the two baths. The interatomic coupling within the lead K is significantly larger than that of the interface coupling.

In our setup, we allow the adjustment of the interatomic distance at the interface, and as a result, the interface coupling can be adjusted. If we stretch the two leads, then the interatomic distance between the leads and within the leads will increase. They will reach a new equilibrium position at the point where $V'(r) = kr$. The interfacial atoms at this new position are balanced by both the Morse potential and the quadratic potential within the lead. However, concerning the

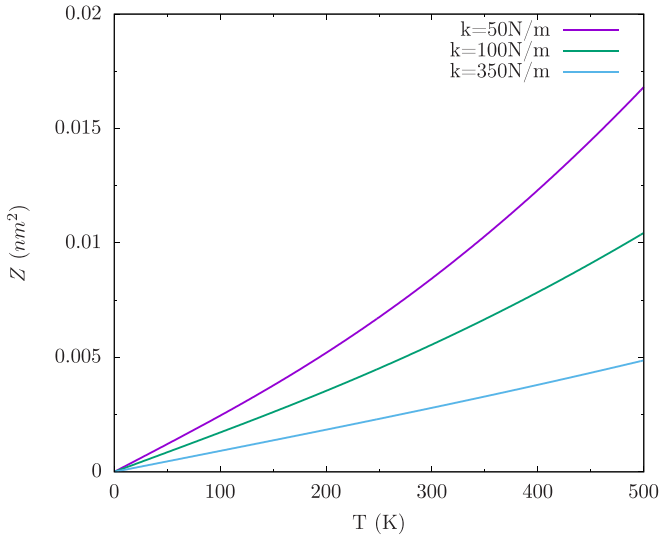

FIG. 3. The mean square of the vibrational amplitude Z is plotted against temperature under different interatomic force constants: $k = 50$ N/m, $k = 100$ N/m, and $k = 350$ N/m.

interface coupling, both the second-order and higher-order force constants are adjusted. The quadratic and fourth-order IFCs can be calculated via the calculations of the derivatives of Morse potential with respect to the new equilibrium position.

Figure 3 shows the temperature dependence of Z, which can be regarded as the mean square of the vibrational amplitude of interfacial atoms. It is seen that Z increases with the increase in temperature. Theoretically, it will eventually linearly increase with respect to temperature in the high-temperature regime. Figure 3 also shows that Z is larger when k is smaller. The magnitude of Z in comparison with the ratio of fourth-order and second-order IFCs ($\eta = T/K$) will determine how important the fourth-order potential is for the elastic scattering processes. If Z is comparable to η, the impact of fourth-order IFCs will have a comparable effect on the elastic scattering processes with respect to the quadratic IFCs. Hence, we can conclude the following: (1) Localized phonons are less important in the low-temperature regime and become increasingly important with the increase in temperature. This result is consistent with previous findings [21]. (2) Localized phonons are more important when the interatomic bonds in the baths are weaker (smaller k) but less important when the bonds are stronger. This is also consistent with the previous studies showing that elastic scattering normally dominates for phonons in graphene, in which the carbon-carbon bonds are strong [22].

Figure 4 shows the temperature-dependent contribution of extended modes to the interfacial thermal conductance, with and without considering the collisions with the localized modes. Here, we have used the interatomic distance at the interface to adjust the potential. We find that localized phonons can both enhance and inhibit the elastic scattering processes, depending on the distance and temperature. When $r = 0.4$ nm, the fourth-order potential suppresses the elastic scattering process at a low temperature but enhances it at a high temperature with a crossover temperature at around $T = 300$ K. When $r = 0.5$ nm, localized phonons suppress

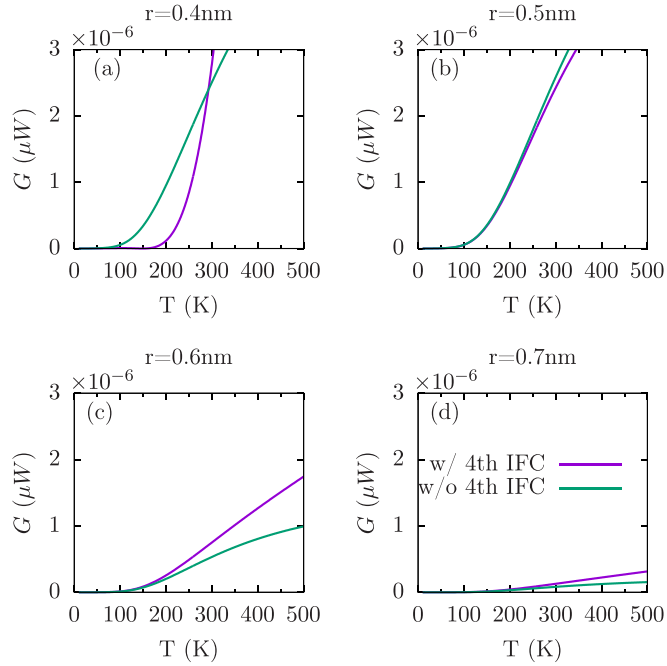

FIG. 4. Temperature-dependent thermal conductance with or without considering the localized phonons at different distances. Parameters: $a = 1/\text{Å}$, $D_e = 0.5$ eV, $k = 350$ N/m, and $r_e = 0.3$ nm.

the elastic scattering process, while at $r = 0.6$ nm and $r = 0.7$ nm, they enhance the elastic scattering process. In this particular one-dimensional model, the effect is determined by the sign of the second-order and fourth-order IFCs. Specifically, when $r = 0.5$ nm, the localized phonons will suppress the elastic scattering process when the sign of the fourth-order IFC is different from that of the second-order IFC. For $r = 0.4$, 0.6, and 0.7 nm, the localized phonons will enhance the elastic scattering since the sign of the fourth-order IFC is the same as that of the second-order IFC. It is noted that with the increase of lead-lead distance, the interfacial coupling decreases exponentially, as seen from the Morse potential, and as a result, the thermal conductance decreases dramatically.

IV. CONCLUSION

In this work, we studied the interactions of extended phonons and localized phonons and their effects on interfacial thermal conduction across a weakly interacting interface. For heat conduction at the interface without localized phonons, phonons with extended modes are heat carriers responsible for interfacial thermal conductance. However, in the presence of fourth-order interatomic potential, phonons with extended modes will collide with the localized phonons, and through such collisions, the localized phonons can significantly affect the transmission of phonons with extended modes. This effect becomes increasingly significant with the increase in temperature. From our model calculation, we show that the localized modes can either enhance or suppress the elastic scattering processes, depending on the coupling coefficients and temperature. This work suggests that in order to accurately evaluate phonon transmission across an interface, one needs to consider the effects of localized phonon modes, especially when the temperature is high.

ACKNOWLEDGMENTS

This work was supported by the National Research Foundation, Singapore, under Award No. NRF-CRP24-2020-0002. Y.-W.Z. acknowledges the support from a Singapore A*STAR SERC CRF Award. The use of computing resources at the A*STAR Computational Centre and National Supercomputer Centre, Singapore, is gratefully acknowledged.

[1] G. Chen, Int. J. Therm. Sci. **39**, 471 (2000).
[2] N. Li, J. Ren, L. Wang, G. Zhang, P. Hänggi, and B. Li, Rev. Mod. Phys. **84**, 1045 (2012).
[3] P. Zhang, P. Yuan, X. Jiang, S. Zhai, J. Zeng, Y. Xian, H. Qin, and D. Yang, Small **14**, 1702769 (2018).
[4] A. Giri and P. E. Hopkins, Adv. Funct. Mater. **30**, 1903857 (2020).
[5] K. Gordiz and A. Henry, J. Appl. Phys. **119**, 015101 (2016).
[6] K. Gordiz and A. Henry, Sci. Rep. **6**, 23139 (2016).
[7] T. Beechem, S. Graham, P. Hopkins, and P. Norris, Appl. Phys. Lett. **90**, 054104 (2007).
[8] J.-S. Wang, J. Wang, and N. Zeng, Phys. Rev. B **74**, 033408 (2006).
[9] J.-S. Wang, J. Wang, and J. T. Lü, Eur. Phys. J. B **62**, 381 (2008).
[10] H. Yang, Y. Tang, and P. Yang, Nanoscale **11**, 14155 (2019).
[11] F. VanGessel, J. Peng, and P. W. Chung, J. Mater. Sci. **53**, 5641 (2018).
[12] R. Qi, R. Shi, Y. Li, Y. Sun, M. Wu, N. Li, J. Du, K. Liu, C. Chen, J. Chen, F. Wang, D. Yu, E.-G. Wang, and P. Gao, Nature (London) **599**, 399 (2021).
[13] Z. Cheng, R. Li, X. Yan, G. Jernigan, J. Shi, M. E. Liao, N. J. Hines, C. A. Gadre, J. C. Idrobo, E. Lee, K. D. Hobart, M. S. Goorsky, X. Pan, T. Luo, and S. Graham, Nat. Commun. **12**, 6901 (2021).
[14] T. Feng, Y. Zhong, J. Shi, and X. Ruan, Phys. Rev. B **99**, 045301 (2019).
[15] B. Xu, S. Hu, S. W. Hung, C. Shao, H. Chandra, F. R. Chen, T. Kodama, and J. Shiomi, Sci. Adv. **7**, eabf8197 (2021).
[16] Y. Chalopin and S. Volz, Appl. Phys. Lett. **103**, 051602 (2013).
[17] Y. Zhou and M. Hu, Phys. Rev. B **95**, 115313 (2017).
[18] H. Zhou, G. Zhang, J.-S. Wang, and Y.-W. Zhang, Phys. Rev. B **101**, 235305 (2020).
[19] H. Li, B. K. Agarwalla, and J.-S. Wang, Phys. Rev. E **86**, 011141 (2012).
[20] P. E. Hopkins, J. Appl. Phys. **106**, 013528 (2009).
[21] K. M. Reid, H. D. Pandey, and D. M. Leitner, J. Phys. Chem. C **123**, 6256 (2019).
[22] A. A. Balandin, ACS Nano **14**, 5170 (2020).